Evidence for Retro-Translocation of Pokeweed Antiviral Protein from Endoplasmic Reticulum into Cytosol and Separation of Its Activity on Ribosomes from Its Activity on Capped RNA†

Bijal A. Parikh,‡,§ Ulku Baykal,§ Rong Di,§ and Nilgun E. Tumer*,‡,§

Biotechnology Center for Agriculture and the Environment and the Department of Plant Biology and Pathology Cook College, and the Graduate Program in Microbiology and Molecular Genetics, Rutgers University, New Brunswick, New Jersey 08901-8520

Received August 20, 2004; Revised Manuscript Received November 3, 2004

ABSTRACT: Pokeweed antiviral protein (PAP) is a single-chain ribosome inactivating protein (RIP) that binds to ribosomes and depurinates the highly conserved α-sarcin/ricin loop (SRL) of the large subunit rRNA. Catalytic depurination of a specific adenine has been proposed to result in translation arrest and cytotoxicity. Here, we show that both precursor and mature forms of PAP are localized in the endoplasmic reticulum (ER) in yeast. The mature form is retro-translocated from the ER into the cytosol where it escapes degradation unlike the other substrates of the retro-translocation pathway. A mutation of a highly conserved asparagine residue at position 70 (N70A) delays ribosome depurination and the onset of translation arrest. The ribosomes are eventually depurinated, yet cytotoxicity and loss of viability are markedly absent. Analysis of the variant protein, N70A, does not reveal any decrease in the rate of synthesis, subcellular localization, or the rate of transport into the cytosol. N70A destabilizes its own mRNA, binds to cap, and blocks cap dependent translation, as previously reported for the wild-type PAP. However, it cannot depurinate ribosomes in a translation-independent manner. These results demonstrate that N70 near the active-site pocket is required for depurination of cytosolic ribosomes but not for cap binding or mRNA destabilization, indicating that the activity of PAP on capped RNA can be uncoupled from its activity on rRNA. These findings suggest that the altered active site of PAP might accommodate a narrower range of substrates, thus reducing ribotoxicity while maintaining potential therapeutic benefits.

Pokeweed antiviral protein (PAP)[1] is a 29 kDa ribosome inactivating protein (RIP) isolated from the leaves of the pokeweed plant (*Phytolacca americana*). PAP and other RIPs such as ricin, Shiga toxin from *Shigella dysenteriae*, and Shiga-like toxin from *Escherichia coli* catalytically remove an adenine (A4324) residue from the highly conserved α-sarcin/ricin loop (SRL) of the large rRNA (*1*−*5*). PAP can also remove an additional adenine and a guanine from the SRL (*6*). The depurination of the SRL has been reported to interfere with the elongation factor-2 catalyzed GTP hydrolysis and translocation of the peptidyl-tRNA to the P-site, resulting in inhibition of translation (*4*, *7*). Unlike ricin and Shiga toxin, which are AB-toxins that consist of an active (A) and a binding (B) chain, PAP is a single chain or type I RIP that consists of only the A chain. The most important feature that separates PAP from ricin is its ability to inhibit virus infection (*8*). The antiviral activity of PAP could be demonstrated without a significant reduction in host cell translation (*9*−*11*). PAP mutants that do not depurinate ribosomes inhibit viral infection, indicating that the antiviral activity can be dissociated from ribosome depurination (*12*, *13*). A few other RIPs also share this activity, yet the mechanism of none has been extensively probed.

RIPs have become important agents in medicine mainly by virtue of their cytocidal properties against cancer cells (*14*−*16*). PAP and ricin have been used as the cytotoxic component of immunotoxins directed against cancer cell targets (*14*−*16*). Because of their potent toxicity, RIPs have been used in biological warfare and more recently in bioterrorism (*17*, *18*). Understanding the relationship between the interaction of RIPs with the ribosome and their cellular toxicity is critical for protecting healthy cells from their cytotoxic effects and developing therapeutic responses against their action.

On the basis of its crystal structure, PAP has been divided into three distinct domains: the N-terminal domain (residues 1−69), the central domain (residues 70−179), and the C-terminal domain (residues 180−262) (*19*−*21*). The most conserved sequence among all RIPs is the catalytic or active-site domain, which contains glutamic acid at position 176 (Glu177 in ricin) and arginine at position 179 (Arg180 in

† This work was supported by National Science Foundation Grants MCB-0348299 and MCB-0130531 to N.E.T.

* Corresponding author. Tel: (732) 932-8165 ext 215. Fax: (732) 932-6535. E-mail: tumer@aesop.rutgers.edu.

‡ Graduate Program in Microbiology and Molecular Genetics.

§ Biotechnology Center for Agriculture and the Environment and the Department of Plant Biology and Pathology Cook College.

[1] Abbreviations: PAP, pokeweed antiviral protein; RIP, ribosome inactivating protein; RTA, ricin A chain; ER, endoplasmic reticulum; ERAD, ER-associated protein degradation; SRL, α-sarcin/ricin loop; rRNA, ribosomal RNA; MHC, major histocompatibility complex; SD medium, synthetic dropout medium; Dpm1, dolichol phosphate mannose synthase; Pgk1, phosphoglycerate kinase; G6PD, glucose-6-phosphate dehydrogenase; CHX, cycloheximide; PMSF, phenyl-methylsulfonyl fluoride.

10.1021/bi048188c CCC: $30.25
Published on Web 01/28/2005

ricin) (*22*−*24*). In the three-dimensional structure, there is a prominent cleft at the interface between the central and the C-terminal domains, which forms the putative substrate binding site (*20*). The amino acids Tyr72 and Tyr123 form a stacking interaction that maintains the substrate adenine in place for nucleophilic attack by residues in the active site (*19*, *24*, *25*). Modeling analysis of the active-site pocket of PAP predicted that the two tyrosine residues at positions 72 and 123 could accommodate the m^7Gppp-X cap found on mRNA (*26*). Analysis of the interaction between PAP and capped RNAs demonstrated that PAP binds to the cap structure in vitro (*26*). PAP regulates its expression by destabilizing its own mRNA in vivo (*27*). Amino acids that are critical for cytotoxicity of PAP have recently been identified (*28*). Mutations of several residues in the central domain abolished cytotoxicity but did not affect ribosome depurination, indicating that ribosome depurination is not sufficient for cytotoxicity (*28*).

Since the substrates of RIPs are present in the cytosol, they need to be delivered into the cytosol in a catalytically active form. Recent studies indicate that the two chain RIPs such as ricin and Shiga toxin are internalized by endocytosis and subsequently undergo retrograde transport via the Golgi complex to reach the endoplasmic reticulum (ER) lumen from where they enter cytosol using the ER-associated degradation pathway (ERAD) (*29*−*32*). This retro-translocation pathway of AB-toxins is similar to the cellular route used by misfolded proteins (*33*). When proteins are transported from the cytosol into ER and do not fold properly, they are often retro-translocated into the cytosol and degraded by the proteasome (*33*). The retro-translocation pathway is also exploited by certain viruses. Two proteins from the human cytomegalovirus called US2 and US11 trigger retro-translocation and degradation of the heavy chain of the MHC class I molecule, allowing the virus to evade the host immune response (*34*). Subsequent degradation of these proteins in the cytosol requires polyubiquitination, which serves as a signal for recognition by the proteasome. Unlike the other substrates of the retro-translocation pathway, AB-toxins such as ricin and cholera toxin are incompletely degraded in the cytosol by mechanisms that are not completely understood (*35*, *36*). Nothing is known about the intracellular pathways followed by type I RIPs and the mechanism by which they access their intracellular substrate. Since the ribosomal target of PAP is intracellular, the cytotoxic action of PAP requires its translocation across the ER membranes into the cytosol.

In this study, we show for the first time that a single chain RIP is retro-translocated from the ER into the cytosol where it completely escapes degradation by the cellular proteasome machinery and remains stable. Mutation of a single amino acid that is not directly involved in catalytic depurination eliminates the cytotoxicity of PAP. This mutation does not affect the rate of synthesis, processing, or retro-translocation of the protein into the cytosol but inhibits depurination of the cytosolic ribosomes. The mutant protein is able to destabilize its own mRNA, bind to cap, and inhibit cap dependent translation in vitro. These results demonstrate that a conserved residue adjacent to the active-site pocket of a single chain RIP modulates both the initiation of and the consequences of ribosome depurination, by altering the activity of the protein on ribosomes, while maintaining its activity on capped RNA.

MATERIALS AND METHODS

Plasmids. PAP expression plasmids used in this study were described previously (*6*, *27*, *37*). Expression of PAP and the nontoxic PAP variants E176V, N70A, G75D, and L71R was under the control of the galactose-inducible *GAL1* promoter in the YEp351-based high-copy plasmid. The NT616 contained the firefly luciferase cDNA from pLUC0 (*38*) downstream of the *GAL1* promoter in YEp351.

Media and Growth Conditions. Saccharomyces cerevisiae strain W303 (*MATa ade2-1 trp1-1 ura3-1 leu2-3, 112 his3-11, 15 can1-100*) was used for all of the assays. Yeast cells were grown at 30 °C in YPD rich medium (1% yeast extract, 2% peptone, and 2% glucose) or synthetic dropout (SD) medium (0.67% Bacto-yeast nitrogen base) supplemented with the appropriate amino acids (*27*, *38*). For trans depurination analysis, cells were grown for 1 h on SD-Leu,-galactose, washed, and resuspended in either SD-Leu,-galactose or SD-Leu,glucose with 100 μg/mL cycloheximide for a total of 6 h of growth as previously described (*28*).

Structural Analysis of Conserved Residues. Coordinates of the various crystal structures from the Protein Data Bank were used in conjunction with ProteinExplorer v1.982, ConSurf server (*39*), ClustalW (http://www.ebi.ac.uk/ clustalw), ESPript v2.2, and the Expasy web server (http://www.expasy.org). Structures used were as follows: PAP complex with formycin 5′-monophosphate (PDB 1PAG) (*19*); ricin complex with formycin-5′-monophosphate (PDB 1FMP) (*40*); crystal structure of β-luffin (PDB 1NIO) (*41*); crystal structure of saporin (PDB 1QI7) (*42*); and trichosanthin complexed with formycin (PDB 1MRK) (*43*).

Toxicity and Viability. Cells were plated from SD-Leu, raffinose plates to SD-Leu, galactose plates to assess toxicity. Viability was assessed by plating cells on noninducing glucose plates after galactose induction in liquid media. A serial dilution of cells was plated using 20 μL of cells at 0.1 A_{600} unit per mL as the starting concentration. Cells were photographed after 72 h of growth at 30 °C.

Analysis of Protein Expression. Protein from frozen yeast cells harvested during the time course of induction was extracted as described by Hudak et al. (*44*). Total protein from each time point was separated on 15% SDS−PAGE, transferred to nitrocellulose, and probed with affinity-purified anti-PAP polyclonal antibody (1:5000). PAP was visualized by chemiluminescence using the Renaissance kit (PerkinElmer Life Sciences). The blots were then stripped for 30−45 min with 8 M guanidine hydrochloride and reprobed with antibody to dolichol phosphate mannose synthase (Dpm1p; Molecular Probes) (1:2000) and 3-phosphoglycerate kinase (Pgk1p; Molecular Probes) (1:5000).

Cell Fractionation. For immunoblot and pulse-labeling analysis, protein from frozen yeast cells harvested during the time course of induction was extracted as described by Frey et al. (*45*). Briefly, after the addition of an equal volume of low-salt (LS) buffer (20 mM HEPES-KOH, pH 7.6, 100 mM potassium acetate, 5 mM magnesium acetate, 1 mM EDTA, 2 mM dithiothreitol, and 0.1 mM phenylmethylsulfonyl fluoride), yeast protease inhibitor cocktail (Sigma), and acid-washed glass beads (Sigma), cells were vortexed for 1 min and chilled for 1 min on ice for a total of four cycles. Crude lysates were centrifuged at 1200*g* for 2 min. This lysate was then centrifuged an additional 20 min at 18 000*g*.

The pellet was washed once with cold water and resuspended in the original volume of LS buffer. The supernatant and pellet fractions were stored at −80 °C. For pulse-chase analysis, equal A_{600} units of cells were spheroplasted and then lysed according to Kornitzer (*46*).

rRNA Depurination Assay. Ribosomal RNA depurination was assayed by primer extension analysis as described previously (*27*). Extension products were separated on a 7 M urea, 5% polyacrylamide gel and quantified using a Phosphorimager (Molecular Dynamics). The amount of total yeast RNA and rRNA used was determined to be in the linear range of detection by primer extension analysis using yeast ribosomes treated with PAP in vitro.

In Vivo [^{35}S] Methionine Incorporation. Yeast cells were grown to an A_{600} of 0.6 in SD-Leu, -Met, 2% raffinose. Cells were then resuspended at an A_{600} of 0.3 in 2% galactose to induce PAP expression. At time zero, [^{35}S] methionine was added to cells growing on galactose. Thirty minutes after pulse labeling, 800 μL of yeast cells were removed for measurement of growth, and additional aliquots of 800 μL were assayed for [^{35}S] methionine incorporation in duplicate as previously described (*27*).

Metabolic Labeling. Metabolic pulse labeling was conducted as described in ref *46*. Yeast cells were grown at 30 °C in SD-Leu, -Met, 2% raffinose to a starting A_{600} of 0.6. At the indicated times, cells were harvested and resuspended in 10 mL of SD-Leu, -Met, 2% galactose at an A_{600} of 0.6, and 0.5 mCi of [^{35}S] methionine/cysteine labeling mix (Express; PerkinElmer) was added. Cells were incubated at 30 °C for 5 min, pelleted, washed once with ice-cold water, and immediately frozen in a dry ice/ethanol bath. For subsequent chase analysis, cells were resuspended in SD -Leu +Met/Cys (0.1% w/v each) and glucose and pelleted at the times indicated. Total cell lysate (either fractionated or unfractionated) was immunoprecipitated using polyclonal anti-PAP antibody (*46*). For metabolic pulse labeling, equal counts were separated on 15% SDS−PAGE gels, while for pulse-chase analysis of fractionated samples, equivalent A_{600} units were separated. Following electrophoresis, the gels were incubated with EN^{3}HANCE (Perkin-Elmer), equilibrated in 10% PEG (MW8000) to prevent cracking, dried, and exposed to BioMax MS (Kodak) film with an intensifying screen at −70 °C for up to 4 days. The gels were subsequently exposed, and the bands were quantified using a Phosphorimager (Molecular Dynamics). [^{35}S] Methionine-labeled in vitro translation products were used as size markers for full-length and mature PAP, respectively.

Microsome Isolation and Proteinase Protection. To isolate spheroplasts, cells (30 OD_{600} units) were harvested by centrifugation at room temperature. The cell pellet was resuspended to 50 OD_{600}/mL in freshly made 100 mM Tris-HCl pH 9.4, 10 mM DTT for 10 min at room temperature (RT). The cells were pelleted again and resuspended to 50 OD_{600}/mL in 1.2 M sorbitol, 50 mM potassium acetate, and 20 mM Tris-HCl pH 7.5, and 1 mg/mL Lyticase (Sigma) was added. The cell suspension was incubated at 30 °C for 30 min. The spheroplasts were pelleted at 2000*g* for 5 min and resuspended to 20 OD_{600}/mL in 0.1 M sorbitol, 50 mM potassium acetate, 20 mM Tris-HCl, pH 7.5, and 1 mM phenyl-methylsulfonyl fluoride (PMSF). The cell suspentions were lysed with 15 strokes of dounce homogenizer. The unbroken cells were removed by centrifugation at 1000*g* for 5 min. The membranes were pelleted at 20 000*g* for 10 min. The pellet was resuspended in 300 μL of membrane storage buffer (250 mM sorbitol, 50 mM potassium acetate, 20 mM Tris-HCl, pH 7.5). To assay for proteinase sensitivity, 20 μL of the membrane suspension was treated with or without 100 μg/mL proteinase K (Fisher Scientific) or 100 μg/mL proteinase K and 2% TritonX-100. All treatments were performed on ice for 30 min and were stopped with 5 mM PMSF. The proteins (10 μL) were separated on a 15% SDS−PAGE and subjected to immunoblot analysis using polyclonal anti-PAP IgG (1:5000) and anti-Kar2 (1:45 000) antibodies.

In Vitro Translation. Transcription of capped luciferase mRNA was performed using *DraI* linearized pLUC0 (*38*) with the appropriate transcription cocktail (Epicenter). Capped mRNA was further purified through a G50 column (AmershamBiosciences) to remove the unincorporated cap analogue. The translation reaction was performed in a nuclease treated yeast translation system according to Iizuka and Sarnow (*47*). Luciferase expression was quantified using a Turner Designs TD-20/20 Luminometer with the luciferase assay system (Promega).

Real-Time PCR Analysis. Total RNA was isolated from yeast using the traditional hot-phenol method as previously described (*27*). cDNA was synthesized from 1 μg of total RNA using random primers and Superscript II (Invitrogen). Real-time PCR was performed using PAP-specific primers (5′GGGTAAGATTTCAACAGCAATTCA-3′ and 5′-CACCACTGGCATCCACTAGCT-3′) or glucose-6-phosphate dehydrogenase (G6PD)-specific primers (5′-CAGCAATGACTTTCAACATCGAA-3′ and 5′-CCGGCACGCATCATGAT-3′) and SYBR green and normalized to a standard curve of known quantity using the ABI 7000 Sequence Detection System (Applied Biosystems).

Purification of PAP and PAP Mutants from Yeast. PAP and PAP mutants were purified from 100 mL of yeast cells after 6 h induction by galactose. The protocol described by Iizuka and Sarnow (*47*) was followed. The cells were harvested at 3000 rpm for 5 min and washed three times with 10 mL of cold WCE-Mannitol buffer (WCE: 30 mM HEPES, pH 7.4, 100 mM potassium acetate, 2 mM magnesium acetate, and 2 mM dithiothreitol; 8.5% w/v Mannitol). For every 1 g of yeast cells, 1 mL of cold WCE-Mannitol-PMSF (0.5 mM PMSF) and 3 g of glass beads (0.5 μM) were added. Yeast cells were vortexed for 30 s followed by 30 s on ice for a total of eight cycles. Cell debris was removed by centrifugation for 10 min at 6500 rpm. The cleared lysate was centrifuged again at 50 000 rpm for 30 min in a Beckman Tabletop ultracentrifuge to get rid of ribosomes, lipids, and insoluble materials. A Sephadex G-25 superfine gel (Amersham Biosciences) column (2 mL bed volume) was prepared by the resin being soaked in WCE-PMSF overnight and washed four times with WCE-PMSF. A total of 250 μL of clarified lysate was added to the column and centrifuged at 1000 rpm for 2 min. The proteins were eluted from the column with WCE-PMSF by being centrifuged at 1000 rpm for 3 min and concentrated with Microcon YM-10 columns (Millipore).

Purification of PAP and PAP Mutants from E. coli. Recombinant PAP and PAP mutants were expressed as N-terminal His-tagged fusion proteins in *E. coli* BL21(DE3)-pLysS cells. Cultures at an A_{600} of 0.6 were induced with 1

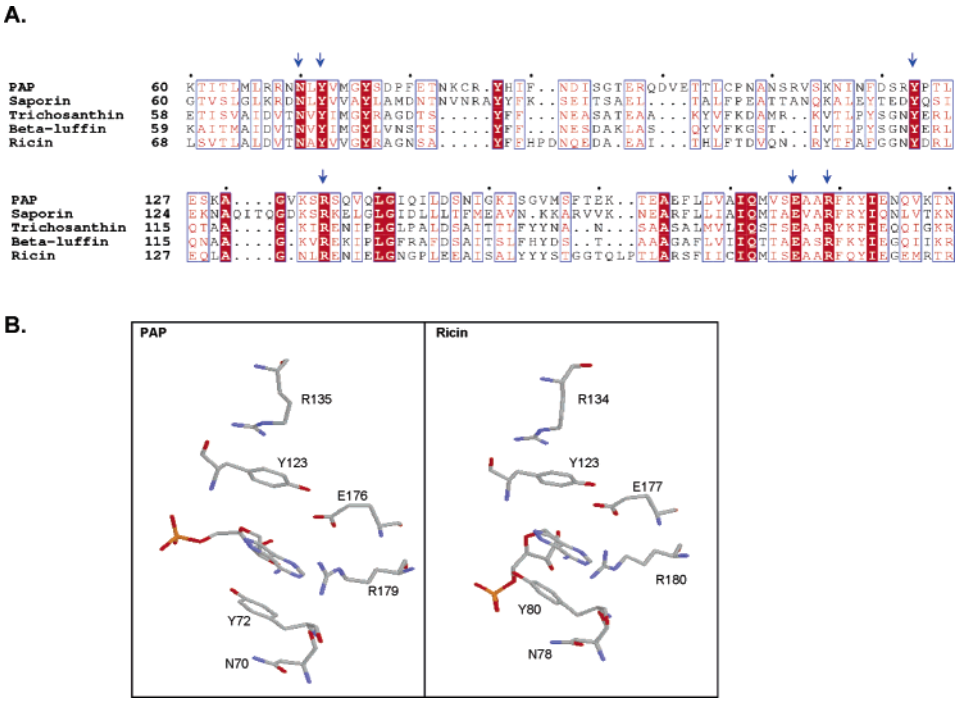

FIGURE 1: Sequence comparison and structural alignment of conserved residues in PAP and other RIPs. (A) Alignment of sequences of five different RIPs with known crystal structures using ClustalW. The N- and C-terminal sequences are not shown. The conserved residues discussed in the text are indicated with a blue arrow. (B) Crystal structure of PAP and ricin complexed with formycin 5′-monophosphate. Only conserved residues indicated in panel A are shown.

mM isopropyl-1-thio-β-D-galactopyranoside for 2.5 h at 37 °C. Cells were harvested and resuspended in 10 mL of binding buffer (20 mM sodium phosphate, 0.5 M NaCl, pH 7.4). The samples were sonicated on ice for 5 min and clarified by centrifugation (15 000 rpm, 20 min) in an Eppendorf centrifuge. His-tagged PAP and PAP variants were batch-purified using Chelating Sepharose Fast Flow column (Amersham Biosciences) according to the manufacturer's instructions. Proteins were eluted from the resin with 2 mL of 20 mM Na_2HPO_4, 0.5 M NaCl, 0.5 M imidazole (pH 7.4). The eluates were concentrated using Centriplus concentrators (Millipore) and 5 μL of concentrated samples was analyzed on 15% SDS−PAGE.

Affinity Chromatography using m^{7}GTP-Sepharose. Cap-binding assay for N-terminal His-tagged recombinant PAP and PAP variants was performed using m^{7}GTP-Sepharose affinity chromatography as described previously (*26*). A total of 15 μL of m^{7}GTP-Sepharose beads (Amersham Biosciences) was incubated with 900 μL of buffer A (20 mM HEPES pH7.4, 200 mM KCl, 2 mM $MgCl_2$) containing 1% BSA. The resin was then washed 3 times with 900 μL of buffer A plus 0.1% Triton X-100. PAP and PAP variants (10 μg) were incubated with the resin overnight in buffer A. The resin was washed again 3 times with 900 μL of buffer A plus 0.1% Triton X-100, and bound proteins were eluted with 30 μL of 0.5 mM m^{7}GTP (Ambion) in buffer A. Aliquots (15 μL) of the eluted fraction were resolved on 15% SDS−PAGE and analyzed by immunoblot analysis as described previously.

RESULTS

Conserved Residues Are Present Adjacent to the Aromatic Ring Structure in the Active Site Cleft of PAP. We used the three-dimensional structure of PAP to extrapolate the importance of conserved residues located near the catalytic site. Using the ConSurf program (*39*), we were able to identify residues located near the active site of PAP that were conserved in over 90% of homologous proteins. A ClustalW alignment, shown in Figure 1A, of several of these proteins demonstrated that the conserved residues are scattered throughout the primary sequence. For example, the two most highly conserved residues in the active site cleft of PAP are Glu176 and Arg179. The tyrosines, Tyr72 and Tyr123, that form a structure analogous to the cap-binding pocket of initiation factor 4E (eIF4E) (*48*) are also highly conserved. Additionally, the structure indicated conservation of amino acids that lie in close proximity to the tyrosine residues, specifically of Asn70 and Arg135 in PAP. The structures of PAP and ricin are shown in Figure 1B where the conserved amino acids marked with arrows in Figure 1A are highlighted. Since not all RIPs are antiviral (*8*−*11*), we hypothesized that Asn70 might in fact modulate the toxicity of PAP without altering its activity on mRNA or viral RNA. We tested the importance of this highly conserved polar residue in the structure of PAP by changing it to alanine.

Cytotoxicity and Loss of Viability Are Affected in N70A. We have previously shown that upon induction in yeast, wild-type PAP inhibited growth while the active-site mutant, E176V, did not (*27*). The initial screen for N70A revealed a lack of cytotoxicity on media containing galactose (Figure 2A). We then assayed for irreversible growth inhibition by conducting viability assays by plating cells on glucose plates after galactose induction for different times in liquid media. As shown in Figure 2B,C, PAP expression reduced the viability of cells by almost 3 logs at 10 h as compared to E176V. In contrast, N70A displayed only a minimal loss of viability at 10 h post-induction. These results indicated that Asn70 is critical for cytotoxicity.

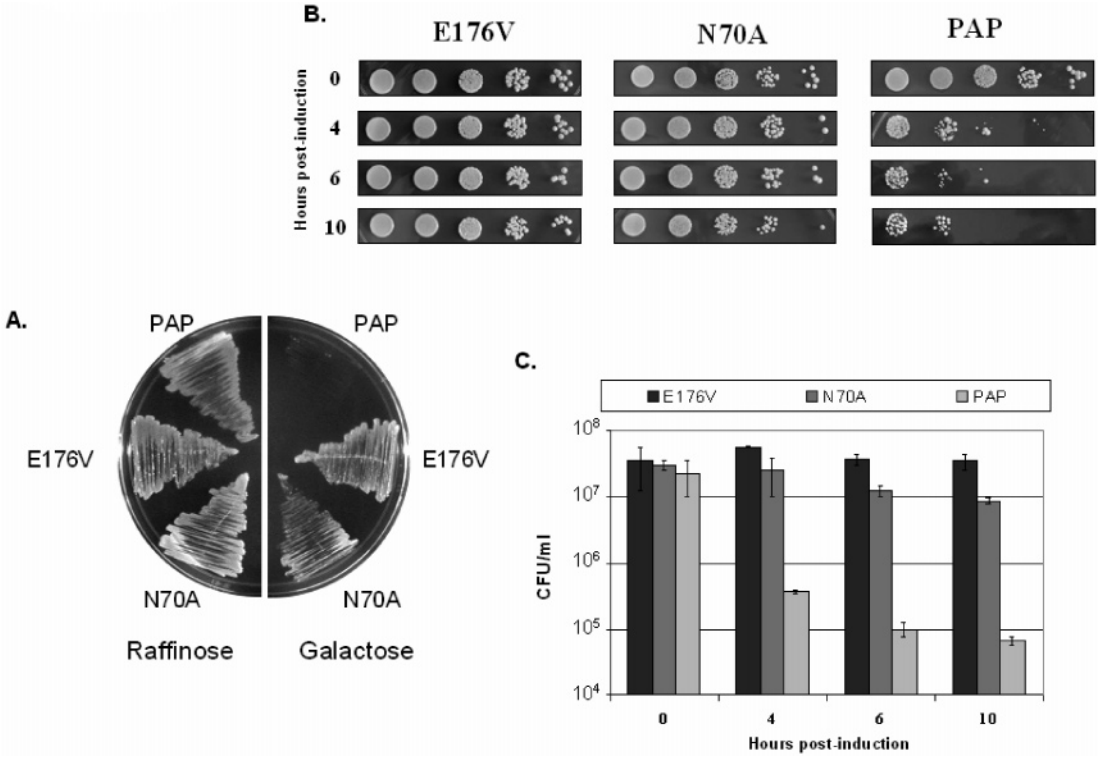

FIGURE 2: Cytotoxicity and viability of PAP, N70A, and E176V. (A) Cells were plated on solid media containing either raffinose or galactose and incubated at 30 °C for 48 h. (B) Cells were induced for the hours indicated in SD-Leu liquid media containing galactose, and serial dilutions were plated on noninducing SD-Leu plates containing glucose. (C) Colony forming units (CFU) per mL were plotted for yeast expressing the PAP mutants shown in panel B. The data represents two independent analyses both done in duplicate.

Ribosome Depurination and Translation Inhibition Are Delayed in N70A. To determine if reduced cytotoxicity of N70A is due to reduced depurination of ribosomes, we investigated the temporal pattern of ribosome depurination by N70A. We have previously shown that depurination in cells expressing wild-type PAP increased rapidly by 4 h post-induction then decreased gradually over time (*27*). Upon galactose induction of N70A in yeast cells, we isolated total RNA and analyzed the rRNA for depurination. We determined the extent of depurination using a previously described dual primer extension assay by comparing amounts of primer extension products synthesized from a primer binding 73 nt downstream of the depurination site and another primer binding 100 nt downstream of the 5′ end of 25S rRNA (*27*). The results shown in Figure 3A indicate a marked delay in depurination in cells expressing N70A as compared to the wild-type protein. As shown by the quantification in Figure 3B, ribosome depurination by wild-type PAP peaks by 4 h and gradually returns to a lower level. Contrary to this, N70A progressively depurinates ribosomes up to 10 h post-induction.

We have previously shown that depurination by wild-type PAP inhibits translation by roughly 70−75% (*27*). To gain a better understanding of the relationship between ribosome depurination and translation arrest, we investigated the temporal pattern of translation inhibition in cells expressing N70A by determining total [^{35}S] methionine incorporation over 30 min at each time interval. The incorporation was normalized to yeast expressing luciferase under the same *GAL1* promoter. As shown in Figure 3C, translation inhibition was near maximal by 4 h post-induction in cells expressing wild-type PAP. This correlated exactly to the peak of ribosome depurination (Figure 3B) and not the extent of depurination. In contrast, N70A did not inhibit translation at 4 h after induction, but only after 8 h was the incorporation affected. This was similarly reflected in the lag period prior to the onset of the highest levels of ribosome depurination (Figure 3B). The inactive variant, E176V, did not display such a reduction in translation as previously reported (*27*).

PAP-Mediated Translation Inhibition Is Effective on PAP Synthesis. Previous results demonstrated that N70A inhibits translation and depurinates ribosomes in vivo with a longer lag than the wild-type protein. Additionally, N70A did not inhibit translation in vivo to the same extent as wild-type PAP. Possible explanations for these observations are that N70A may be synthesized at a lower rate than wild-type PAP, it may be processed at a slower rate, or its transport into the cytosol may be reduced.

To assess the rate of production of PAP, we conducted immunoprecipitation analysis of yeast cells pulse labeled with [^{35}S] methionine for 5 min at various times after galactose induction. The results of these studies are shown in Figure 4A and are quantified in Figure 4B. Initially, synthesis of wild-type PAP is detectable (time 0); however, by 4 h no appreciable amount of PAP is seen. This inhibition continues for the duration of the induction and parallels the translation inhibition seen in Figure 3C. The inactive variant, E176V, is continually synthesized and at rather high rates at 4 and 6 h post-induction. The data accurately reflects the lack of translation inhibition with E176V (Figure 3C). N70A, which showed translation inhibition at 8 and 10 h post-induction (Figure 3C), also shows maximal inhibition of protein production at 10 h but not at 6 h or before. The size of the pulse labeled protein corresponds to the precursor form of PAP. Overall, these results demonstrate that PAP-mediated translation inhibition is equally effective on PAP translation

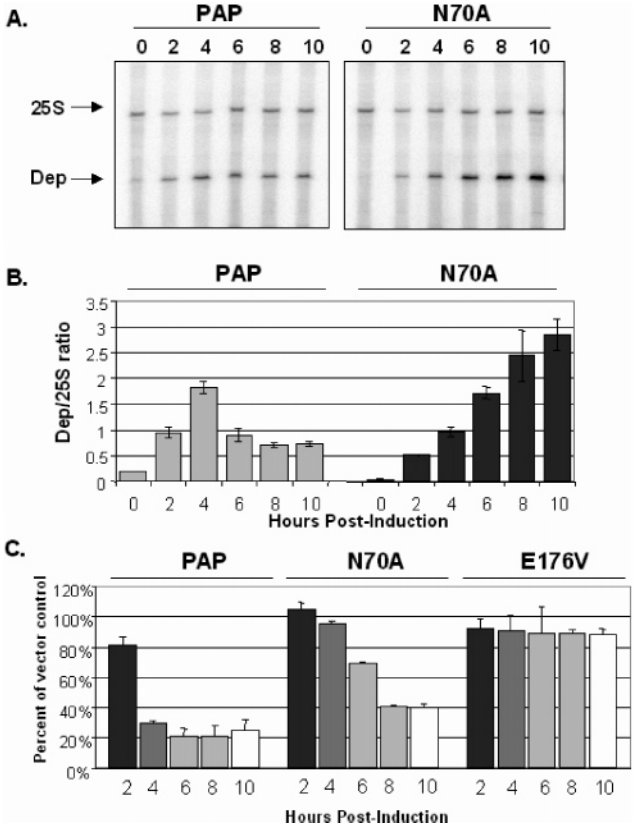

FIGURE 3: Ribosome depurination in yeast expressing PAP and N70A. (A) Primer extension analysis using two different end labeled primers, the depurination primer (Dep) used to measure the extent of depurination and the 25S rRNA primer (25S) used to measure the amount of 25S rRNA. (B) Ratio of Dep/25S shown in panel A. The results represent an average of two independent experiments. The times shown are in hours. (C) Analysis of total translation in yeast. At the times (hours post-induction) indicated, [^{35}S] methionine was added to cells expressing PAP, N70A, and E176V, and 30 min after incubation the extent of [^{35}S] methionine incorporation was determined. The counts obtained were normalized against [^{35}S] methionine incorporation in cells expressing luciferase under the *GAL1* promoter, and the relative incorporation was plotted. The results represent an average of two independent experiments both of which are done in duplicate.

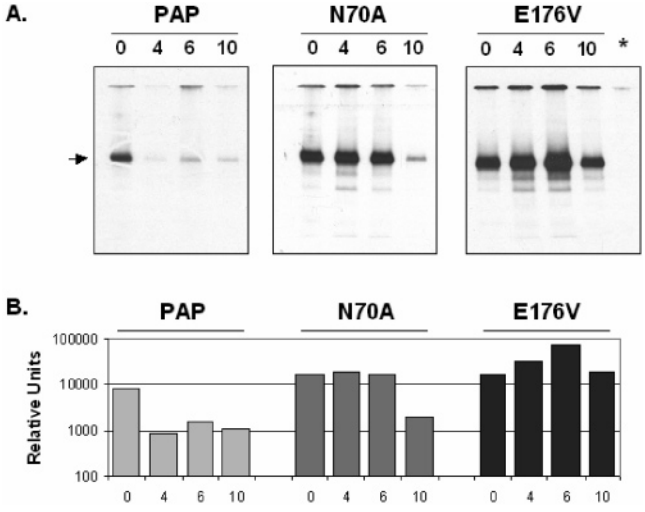

FIGURE 4: Pulse labeling of yeast cells. Cells were grown for indicated times (in hours) in media lacking methionine containing galactose. At the indicated times, the cells were harvested, pulsed for 5 min with [^{35}S] Express in SD-Leu, -Met containing galactose, and immunoprecipitated using polyclonal PAP antibody. (A) Equal counts were loaded on 15% SDS−PAGE and subjected to fluorography. The lane marked with an asterisk indicates N70A cells that were grown on glucose and immunoprecipitated as a control for nonspecific binding. (B) The immunoprecipitated proteins were quantified using a Phosphorimager. The arrow denotes the position of the precursor form of PAP (33 kDa).

as it is on translation of total cellular protein. Furthermore, at no point during induction is the production of N70A less than that of wild-type PAP. Since N70A is synthesized to a similar extent as E176V, we can conclude that the decreased catalytic activity is not due to synthesis at lower rates.

Association of PAP with the Membrane and Cytosolic Fractions. To determine if the decreased activity is due to altered processing and cytoplasmic localization, we have fractionated yeast extracts into cytoplasmic and membrane fractions using a gentle low-salt lysis procedure (*45*). Each fraction was analyzed for the presence of PAP, N70A, and E176V at various times after induction. As controls for the procedure, the integral ER membrane protein dolichyl-phosphate β-D-mannosyltransferase (Dpm1p) and the cytosolic protein phosphoglycerate kinase (Pgk1p) were analyzed in parallel. The results of this steady-state analysis are shown in Figure 5. As expected, Dpm1p segregated with the P18 fraction, while Pgk1p was predominantly in the S18 fraction. Since translation is inhibited after 4 h in cells expressing wild-type PAP, the protein distribution seen beyond 4 h is a result of processing and subcellular redistribution. Although the precursor form was associated with the ER membrane, it was not exclusively found there. The abundance of the precursor form on the membrane decreased with time, as the abundance of the mature form increased. Low level of the precursor form was present in the cytosol. Further studies will address if the precursor form is easily dislodged from the membrane. The precursor form of the protein disappeared from both fractions by 24 h, and there was conversely an increase in the mature processed form in the cytosol only. These results demonstrate that the protein is very stable and that the half-life of the mature form exceeds that of the precursor form, both of which are on the order of hours.

The steady-state expression pattern for E176V indicated accumulation on the membrane fraction, which is likely due to the lack of translation inhibition. The precursor form of E176V was synthesized early, and its synthesis was continued during induction. The abundance of the mature form increased in the cytosol up to 24 h. We have previously reported that the precursor form contains a 22 amino acid signal sequence and 29 amino acid C-terminal extension, which are likely missing in the mature form since it comigrates with purified PAP (*27*). The steady-state cytosolic abundance and distribution of N70A was similar to E176V except that the precursor form accumulated on the membranes up to 6 h post-induction due to lack of translation inhibition. As observed with wild-type PAP, the precursor form disappeared from the cytosolic fraction by 24 h, and there was an increase in the abundance of the mature form in the cytosol. These results demonstrated that the precursor form of PAP accumulated on the ER membranes and the mature form accumulated in the cytosol.

PAP Is Localized in the ER. To investigate the distribution of PAP with respect to the cytosolic and lumenal faces of the ER membrane, we isolated microsomes from yeast expressing wild-type PAP or the mutant forms and assayed

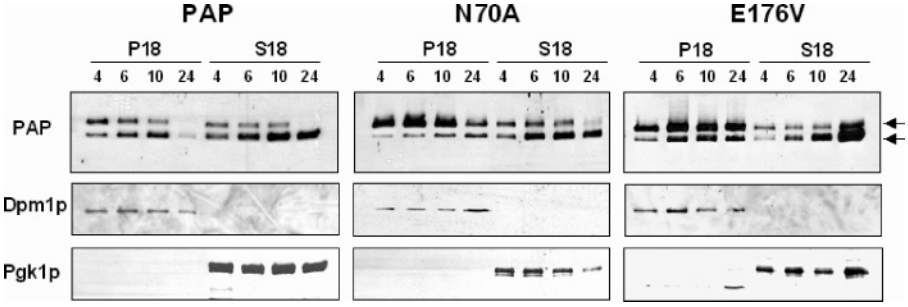

FIGURE 5: Steady-state accumulation of PAP in membrane and cytosolic fractions. Yeast cells were induced for the times indicated (hours), lysed, and fractionated into membrane (P18) and cytosolic (S18) components. Equal amount of total protein (10 μg) was analyzed in each lane. Antibodies against the membrane marker, Dpm1p, and the cytosolic marker, Pgk1p, were used as controls to demonstrate lack of cross-contamination. The arrows indicate the precursor and the mature forms of PAP.

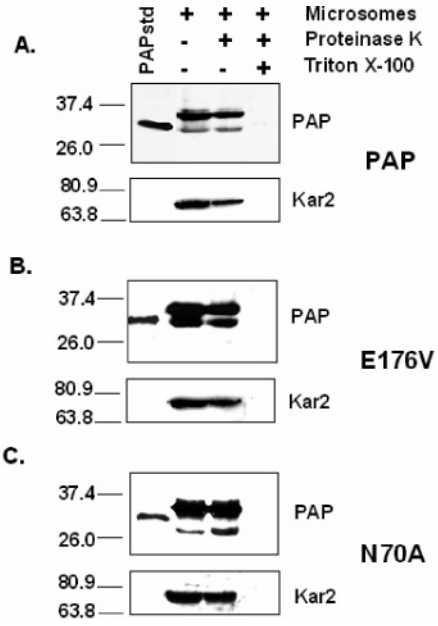

FIGURE 6: Proteinase protection assay. The microsomal pellet from yeast cells expressing wild-type PAP, E176V, and N70A was treated with buffer alone (microsomes), 100 μg/mL proteinase-K, or 100 μg/mL proteinase-K and 2% Triton X-100. After 30 min incubation on ice, 5 mM PMSF was added to each sample, and the samples were subjected to immunoblot analysis using anti-PAP IgG. The N70A fractions (C) were electrophoresed longer than the fractions containing PAP (A) and E176V (B). Each blot was stripped and reprobed with anti-Kar2. Purified PAP (10 ng) was used as standard.

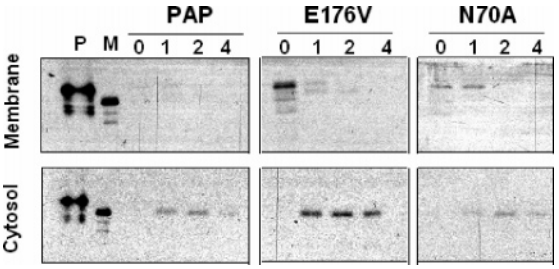

FIGURE 7: Pulse-chase analysis of yeast cells. Cells were pulsed for 5 min with [^{35}S] Express (after 1 h of growth in galactose) in media lacking methionine and chased for the indicated hours in SD-Leu, +Met, +Cys containing glucose immunoprecipitated using polyclonal PAP antibody. Equal A_{600} units were fractionated into membrane and cytosolic fractions, separated on 15% SDS−PAGE, and subjected to fluorography. Lane P indicates the precursor form, and lane M indicates the mature form of PAP synthesized in vitro.

their susceptibility to proteolysis. If PAP is associated with the cytoplasmic face of ER, it will be accessible to protease in a detergent independent fashion. In contrast, if PAP is in the ER lumen, it should only be degradable after solubilization of the ER membrane with a detergent. Microsomal membranes were prepared from spheroplasts isolated from yeast expressing wild-type PAP, E176V, and N70A and subjected to proteinase K digestion in the presence or absence of Triton X-100. As a control, Kar2p, a yeast ER lumenal protein, was used to demonstrate that it is protected from proteolytic activity in the absence of the detergent (Figure 6). In the presence of Triton X-100, Kar2p was susceptible to degradation by proteinase K. Analysis of the microsomal fraction from cells expressing wild-type PAP indicated that the precursor and the mature form of PAP were present in the microsomal pellet (Figure 6A). Both forms of PAP were protected from degradation in the absence of detergent but were degraded by proteinase K in the presence of detergent, demonstrating their transfer across the microsomal membrane. Similar results were obtained with E176V and N70A (Figure 6B,C). We have previously shown that the 22 amino acid signal sequence of PAP is processed when it is translated in vitro in the presence of microsomes (*37*). Therefore, we anticipate that the precursor form localized in the ER is missing its signal sequence and bearing the C-terminal extension, while the mature form in the ER is missing both the signal sequence and the C-terminal extension. The mature form of PAP in the ER migrated slightly faster than the PAP standard, which was more obvious when N70A fractions were electrophoresed longer (Figure 6C). These results demonstrated that the precursor and the mature form of PAP are localized in the ER. Neither form of PAP is protease accessible, indicating that they are predominantly associated with the lumenal face of the ER.

PAP Is Retro-Translocated into the Cytosol. Previous studies indicated that both the precursor and the mature form of PAP are localized in the ER. Since the mature form accumulates in the cytosol during induction, it may be retro-translocated from the ER into the cytosol. To examine this, we carried out a pulse-chase analysis of PAP, E176V, and N70A to determine the half-life, maturation, and localization of newly synthesized protein. Yeast cells were pulsed for 5 min after 1 h of growth on galactose and chased in glucose containing media supplemented with methionine and cysteine to inhibit transcription of new PAP mRNA and any further labeling of PAP. The cells were then fractionated into membrane and cytosolic fractions and immunoprecipitated using PAP antibodies. As shown in Figure 7, the precursor form of the wild-type PAP was barely detectable in the membrane fraction after 1 h of growth on galactose (lane

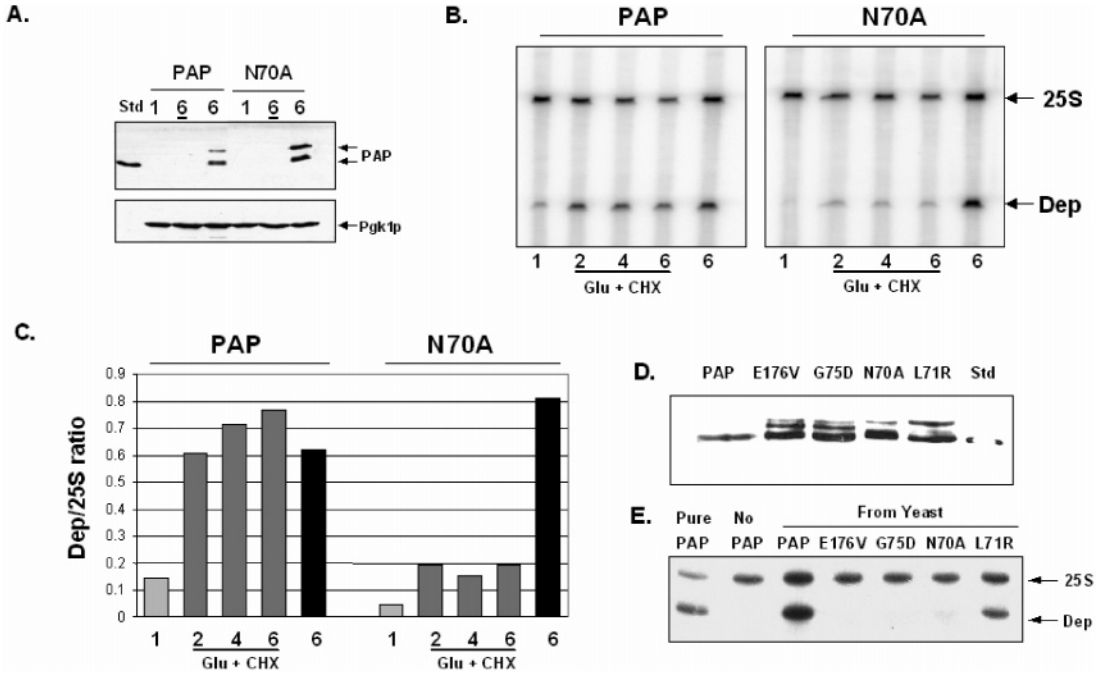

FIGURE 8: Ribosome depurination in yeast in vivo and in vitro. The underlined times (in hours) indicate addition of cycloheximide and glucose after the first hour of induction (Glu + CHX). (A) Immunoblot analysis indicating the level of PAP present at 1 and 6 h after induction (lanes labeled 1 and 6) and at 6 h after shut-off of PAP transcription and translation (lanes labeled 6). Purified PAP (10 ng) was used as standard. Total protein (10 μg) was analyzed in each lane. The blot was stripped and reprobed with anti-Pgk1 to show equal loading. (B) Primer extension analysis using two different end labeled primers, the depurination primer (Dep) used to measure the extent of depurination and the 25S rRNA primer (25S) used to measure the amount of 25S rRNA in vivo. (C) Ratio of Dep/25S from panel B. The results were confirmed at least twice. The extent of depurination was in the linear range of detection (not shown). (D) PAP and PAP mutants extracted from yeast and used in the depurination assay shown in panel E. Purified PAP (10 ng) was used as the standard. (E) PAP and PAP mutants extracted from yeast were incubated with ribosomes from wild-type yeast in vitro, and the extent of depurination was determined by primer extension analysis.

0). The mature form of PAP appeared in the cytosol after 1 h of chase (lane 1), indicating rapid retro-translocation into the cytosol. The precursor from of E176V was observed in the membrane fraction after 1 h of growth on galactose (lane 0), and the mature form appeared in the cytosol after 1 h of chase (lane 1). Only the precursor form was found in the ER fraction and the mature form was found exclusively in the cytosol. The precursor form of the newly synthesized N70A was observed in the membrane fraction, and the mature form was observed in the cytosol after 1 h of chase (lane 1). The precursor form of N70A was retained in the membrane fraction somewhat longer than the wild-type PAP. However, the appearance of the mature form in the cytosol followed the same kinetics as the wild-type PAP and E176V. These results indicated that the mature form of PAP is retro-translocated from the ER into the cytosol.

Asn70 Plays an Important Role in Facilitating Depurination in Trans. The temporal pattern of depurination and translation arrest in N70A suggested a reduced affinity for the ribosomes. However, eventually ribosomes are depurinated possibly due to increased amounts of protein synthesized. This implies that the mutation of Asn70 decreased the catalytic activity of the protein, and the ribosomes may now be attacked in a stoichiometric fashion rather than in a catalytic fashion.

To test this hypothesis, we designed an assay in which we could test the efficacy of depurination in trans. We have already demonstrated that wild-type PAP can depurinate ribosomes in trans in yeast cells (*27*). We induced either PAP or N70A expression for 1 h, to prevent the accumulation of large amounts of protein. We have previously shown that 1 h induction does not appreciably depurinate ribosomes in yeast, most likely due to a delay in processing and transport of protein (*27*). We have used the amount of depurination at 1 h as a baseline and determined the efficacy of further depurination (depurination in trans) above this baseline by monitoring the catalytic activity after shutting off transcription and translation by growing cells in media containing glucose and cycloheximide. As shown in Figure 8A, immunoblot analysis confirmed that undetectable levels of protein were present after either a 1 h induction (lanes labeled 1) or a 1 h induction followed by 5 h of growth in media containing glucose and cycloheximide (lanes labeled 6). In contrast, equally high levels of protein were seen after the typical 6 h induction (lanes labeled 6). The primer extension analysis is shown in Figure 8B and quantified in Figure 8C. Wild-type PAP depurinated ribosomes in trans when transcription and translation were shut off (lanes labeled Glu + CHX). In contrast, N70A was less efficient in conducting trans depurination than wild-type PAP (lanes labeled Glu + CHX). The level of trans depurination observed with N70A was 20−25% of the total depurination observed after 6 h of growth on galactose (lane labeled 6). After 6 h of growth on galactose, a higher level of depurination was observed with N70A as compared to wild-type PAP (lane labeled 6). These results indicated that N70A cannot depurinate ribosomes in trans in a translation independent manner.

To determine if N70A can depurinate ribosomes in vitro, we extracted the mutant protein from yeast and treated yeast ribosomes in vitro with the mutant protein. A previously

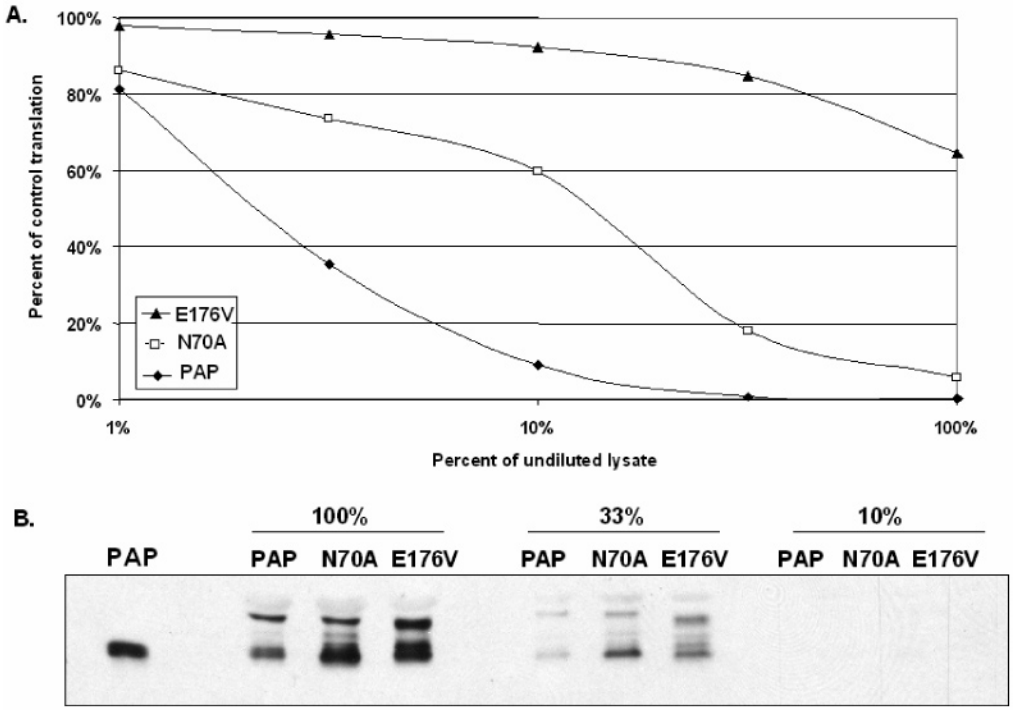

FIGURE 9: In vitro translation in yeast lysates. (A) PAP, N70A, or E176V extracted from yeast after 4 h of induction was added to a yeast S30 translation system charged with capped luciferase mRNA. Translation was expressed as the relative light units (RLU) after 1 h of incubation at 25 °C and normalized against extract without any additional protein added. (B) The relative abundance of PAP in the indicated dilutions of the lysate is shown by immunoblot analysis. Purified PAP (10 ng) was used as a standard.

described dual primer extension analysis was carried out to determine the extent of depurination. Figure 8D shows the amount of protein used in the depurination assay, which is shown in Figure 8E. Wild-type PAP extracted from yeast depurinated ribosomes. In contrast, N70A extracted from yeast did not depurinate ribosomes. The active site mutant, E176V, and a previously described mutant, G75D, which does not bind ribosomes (*49*), did not depurinate ribosomes in vitro. Another mutant, L71R, which depurinates ribosomes in trans and inhibits translation (*28*), depurinated ribosomes in vitro. These results provided further evidence that N70A has a defect in catalytic depurination of the ribosomes.

N70A Inhibits Translation in Vitro, But to Lower Extent than Wild-Type PAP. We previously detected a lack of translation inhibition at 4 h post-induction in cells expressing N70A as compared with a 60−70% reduction by wild-type PAP (Figure 3C). Furthermore, we observed reduced depurination in trans, suggesting a decrease in catalytic activity. Since Asn70 is within the active site cleft of PAP and is highly conserved among different RIPs, a mutation in this residue might alter the active site of the protein such that it is not catalytically active. To determine if the reduced catalytic activity at 4 h post-induction is due to an alteration of the active site, we investigated whether the protein expressed in yeast at 4 h post-induction was capable of translation arrest in vitro. Protein extracted from yeast at 4 h post-induction was added to an S30 extract from yeast charged with capped luciferase mRNA. Although N70A did not inhibit translation in vivo at 4 h post-induction, N70A extracted from yeast 4 h after induction inhibited translation in vitro (Figure 9A). Almost complete inhibition of capped mRNA was seen when 100% of the extracted protein (around 10 ng) was added to a 20 μL translation reaction. In contrast, E176V extracted from yeast caused only a slight reduction in translation. At increased dilutions of N70A, a difference in affinity was apparent (Figure 9A). Immunoblot analysis shown in Figure 9B demonstrated that slightly higher amount of N70A was used in the translation assay as compared to wild-type PAP, indicating that the reduction in translation inhibition with low concentrations of protein was not a result of decreased protein abundance. These results indicated that N70A synthesized up to 4 h post-induction is capable of inhibiting translation in vitro, indicating that the N70A mutation does not lead to a significant alteration of the active site. Similar results were obtained when these experiments were repeated using the rabbit reticulocyte lysate. Analysis in reticulocyte lysate demonstrated that capped mRNA was inhibited more than uncapped mRNA by N70A (data not shown), as previously demonstrated for purified PAP (*6*).

N70A Binds to Cap and Destabilizes Its Own mRNA. The results shown in Figure 9 confirmed that N70A could inhibit translation in vitro. Since N70A did not depurinate ribosomes in vitro, it may be inhibiting translation by binding to the cap structure. To determine if N70A is capable of binding to cap, we purified histidine tagged N70A, wild-type PAP, and inactive PAP (E176V) expressed in *E. coli* and determined if they bind to m^7GTP-Sepharose. The m^7GTP-Sepharose beads were incubated with the purified proteins, and the bound protein was eluted from the beads with 0.5 mM m^7GTP. Figure 10A shows the histidine tagged proteins purified from *E. coli*, and Figure 10B shows the proteins eluted from the m^7GTP-Sepharose. As shown in Figure 10B, PAP purified from pokeweed bound to m^7GTP-Sepharose as previously reported (*26*). Similarly, histidine-tagged wild-type PAP, as well as N70A and E176V, bound to m^7GTP-Sepharose and eluted with 0.5 mM m^7GTP.

Since the active site of N70A was capable of binding to cap, we wanted to assess whether another activity of the

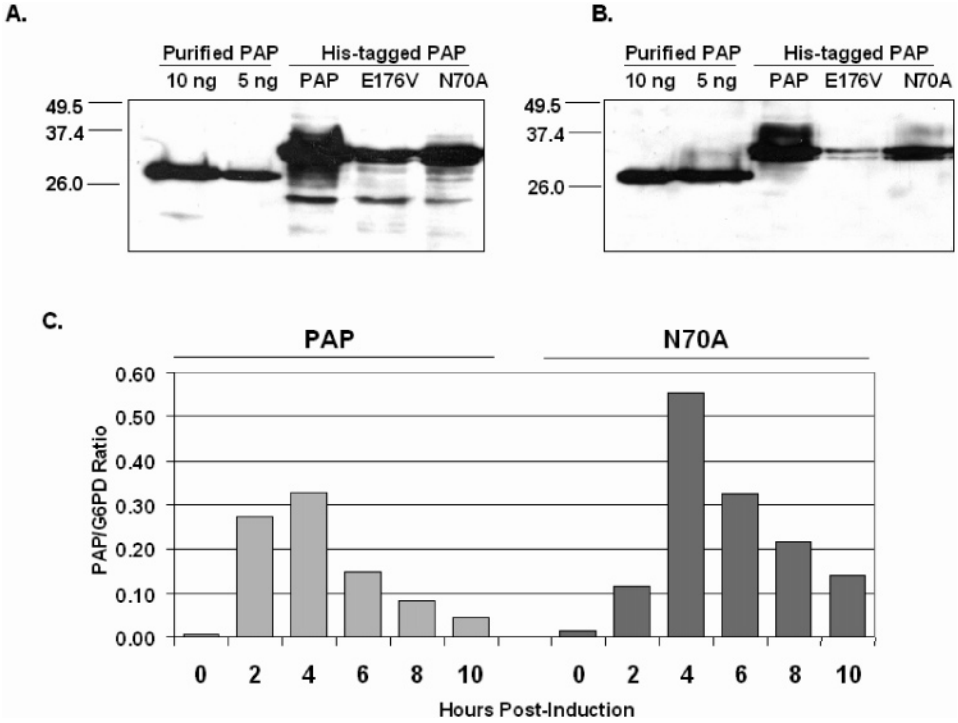

FIGURE 10: Analysis of cap-binding and mRNA abundance. (A) Immunoblot analysis of His-tagged proteins purified from *E. coli*. PAP purified from pokeweed (10 and 5 ng) was used in lanes 1 and 2, respectively. Five μL of each protein purified from *E. coli* was separated on the gel. (B) PAP purified from pokeweed and His-tagged wild-type PAP, E176V, and N70A purified from *E. coli* were incubated with m^7GTP Sepharose and eluted with 0.5 mM m^7GTP. Eluted protein was analyzed by immunoblot analysis using a polyclonal antibody to PAP. (C) Real-time PCR analysis of cells expressing PAP and N70A. Cells were induced for the hours indicated, and total RNA was isolated. Equal amounts of RNA were transcribed into cDNA using random primers, amplified with gene specific primers against PAP or G6PD, and analyzed using the ABI 7000 Sequence Detection System. The results, plotted as a ratio of PAP to G6PD, were reproduced at least twice with either random primed or oligo(dT) primed cDNA.

catalytic center was affected, namely, the destabilization of its own mRNA. We have previously shown that PAP destabilizes its own mRNA by a posttranscriptional mechanism that is independent of translation (*27*). E176V did not destabilize its own mRNA, indicating that the destabilization requires an intact active site (*27*). To determine if N70A destabilizes its own mRNA, we induced expression of wild-type PAP or N70A and isolated total RNA at different times after induction. PAP mRNA levels were quantified by real time PCR using glucose-6-phosphate dehydrogenase (G6PD) mRNA levels as an internal control. As shown in Figure 10C, N70A reduced the steady-state levels of its own mRNA with almost the same temporal pattern as the wild-type PAP. Specifically, the abundance of N70A mRNA increased by 4 h post-induction and decreased subsequently with similar kinetics as in cells expressing wild-type PAP. Similar results were obtained using RNase protection analysis (data not shown). These results indicate that the N70A mutation does not affect cap binding or mRNA destabilization but inhibits catalytic depurination of ribosomes, separating the activity of PAP on ribosomes from its activity on capped RNA.

DISCUSSION

By structural comparison of RIPs, we have identified conserved residues in close proximity to the active site of PAP and analyzed the effect of a mutation in one of these highly conserved residues. The fact that all RIPs analyzed to date contain an asparagine in close proximity to the Tyr72 involved in stacking interactions with the substrate attests to the importance of this residue in the catalytic function of the protein. Since not all RIPs are antiviral (*8*−*11*), we hypothesized that the conserved residue might in fact modulate the toxic consequences of RIP expression without altering its activity on mRNA or viral RNA. We demonstrate here that a mutation in Asn70 modulates ribosome depurination, reducing cytotoxicity without affecting the activity of the protein on its own mRNA.

Cytotoxicity was reduced because ribosome depurination and translation inhibition were delayed by several hours in cells expressing N70A. Ribosomes were eventually depurinated, and translation was inhibited without obvious defects in the mutant protein's synthesis, maturation, abundance, or localization. We have correlated the decrease in translation inhibitory activity to impaired ability to depurinate ribosomes in trans in vivo and in vitro. The asparagine located at position 70 is important not only for PAP but all other RIPs that share conservation of the amino acids surrounding the active site cleft. Although mutation of Asn70 to Ala effectively slowed the process of depurination and translation inhibition, both events still occurred without the concomitant emergence of cytotoxicity or cell death as measured by loss of viability.

Modeling studies indicated that Asn70, which is in the active site cleft and is not directly involved in the catalytic depurination of rRNA, promotes specific interactions with the phosphate backbone of the SRL (*50*). Simultaneous mutations of the polar residues Asn69 and Asn70 were shown to destabilize binding to an oligo corresponding to the SRL in vitro (*51*). This mutant also exhibited reduced affinity for ribosomes and ribosomal protein L3 in vitro (*52*). Thus,

mutation of Asn70 is predicted to disrupt stabilizing interactions with the phosphate backbone of the SRL, affecting catalytic activity of the protein on ribosomes in vivo. Furthermore, X-ray structure analysis indicates that Asn70 forms a hydrogen bond with Arg179 at the active site (*19*), suggesting that a mutation in Asn70 may affect the conformation of the active site to allow differential accommodation of substrates, such that it can accommodate the cap structure, but not the phosphate backbone of the SRL, reducing the activity of PAP on ribosomes without affecting its ability to bind to cap. Asn70 might also be required for interactions with cellular partners that are necessary for catalytic depurination of ribosomes and cell death. The association of the two events suggests that binding to a cellular factor may actually provide a mechanism for PAP to specifically target translating ribosomes.

In previous studies, we uncovered the dual ability of PAP to target not only ribosomes but mRNA as well and showed that PAP binds to the m^7GpppX cap structure (*26*). Modeling studies of cap interaction with PAP predicted that the cap structure would bind to the active site of PAP in a manner similar to adenine of rRNA. The affinity of PAP for cap was only 4-fold lower than its affinity for the SRL, and the methylated cap structure competed with the rRNA for binding to PAP (*26*). The similar affinity of PAP for either the mRNA or the SRL suggested that PAP targets either the rRNA or mRNA, but not both. Biochemical analysis confirmed that the protein has a single binding site (*26*). We obtained in vivo evidence that mRNA is targeted by PAP by demonstrating that PAP affects the abundance of its own mRNA and specific mRNAs in yeast by a mechanism that can be separated from depurination of the rRNA (*27*).

We show here that PAP mRNA levels increase dramatically in yeast expressing N70A at 4 h post-induction as previously observed with the wild-type PAP. We previously thought that inhibition of elongation is responsible for this dramatic increase in PAP mRNA since maximal inhibition of translation was observed at 4 h post-induction. Since we do not observe a significant inhibition of translation at 4 h in cells expressing N70A, the mRNA stabilization observed in these cells is not likely due to inhibition of elongation but may be due to binding of PAP to its own mRNA. As observed with wild-type PAP, mRNA abundance decreased after 4 h in cells expressing N70A, indicating that N70A can destabilize its own mRNA in the absence of ribosome depurination. Total translation is not inhibited in yeast expressing N70A until 8 h after induction, which corresponds to the timing of mRNA destabilization. These results suggest that cap binding may be responsible for inhibition of cap dependent translation and the destabilization of PAP mRNA in cells expressing N70A.

The consequence of ribosome depurination was thought to be the primary trigger for cytotoxicity of RIPs (*9*−*11*). We recently showed that ribosome depurination by itself is not sufficient for cell toxicity (*28*). A mutant form of PAP that depurinated cytosolic ribosomes and inhibited translation, but did not destabilize its own mRNA, was not cytotoxic, suggesting that the activity of PAP on mRNA may also contribute to cytotoxicity (*28*). We show here that in the absence of ribosome depurination, the ability to bind to cap and destabilize mRNA is not sufficient for cytotoxicity. These results suggest that cytotoxicity of PAP may be due to the combined effects of the protein on ribosomes and mRNA, such that disruption of either activity leads to a reduction in cytotoxicity.

Since the targets of AB-toxins are present in the cytosol, they need to be delivered into the cytosol in a catalytically active form. Several bacterial AB-toxins, such as diphtheria toxin and anthrax toxin, enter the cytosol in response to the low pH of the endosomal compartment (*36*). In contrast, the plant toxin ricin and the bacterial toxins cholera and Shiga toxin are transported not only to endosomes but retrograde through the Golgi apparatus and to the ER before the enzymatically active A chain enters the cytosol (*36*). Since this pathway is used by secretory proteins that fail to fold or assemble properly (*53*, *54*), there is evidence that toxins enter this pathway by disguising themselves as proteins with a folding defect (*55*). We show here that a single chain RIP is retro-translocated from the ER into the cytosol upon processing of its N-terminal signal sequence and the C-terminal extension.

A variety of secretory proteins can be imported into the ER posttranslationally in yeast, and it has been shown that the N-terminal signal sequence determines whether a co- or posttranslational pathway is used (*56*). We have previously reported that folding of PAP protein may occur on the ribosome because PAP is able to depurinate ribosomes in a translation dependent manner and the extent of depurination gradually increases with increasing length of the C-terminus (*28*). These results suggest that PAP may associate with the ER membranes in a posttranslational manner. This is further supported by the observation that deletion of the N-terminal signal sequence does not affect the cytotoxicity of PAP or its ability to depurinate ribosomes (*28*). Cytotoxicity and the ability to depurinate ribosomes were lost only after tyrosine at position 16 of the mature protein was deleted (*28*).

The cleavage of the C-terminal extension of PAP may expose a hydrophobic region present at the C-terminus of the mature protein, which may promote unfolding or membrane interaction. We have previously shown that a PAP mutant (PAPc), which is missing 25 amino acids from the C-terminus of mature protein, is nontoxic and does not depurinate ribosomes (*49*). The missing 25 amino acids contain a di-leucine motif that appears to be required for dissociation from ribosomes since the mutant protein remained bound to the ribosomes (*49*). These results suggest that the hydrophobic C-terminal tail of PAP might facilitate its transport across membranes by interaction with ER membrane protein translocators. The mature form of PAP in the ER migrated slightly faster on SDS−PAGE than the standard. This may be due to differences in folding of the protein in the ER versus in the cytosol.

Toxins that are retro-translocated from the ER into the cytosol have an unusually low lysine content. Since lysine residues are potential ubiquitination sites, it has been proposed that the paucity of lysines reduces the chance of ubiquitination and subsequent ubiquitin-mediated degradation (*55*). Results with cholera toxin indicate that poly-ubiquitination is not required for retro-translocation of all proteins across the ER membrane (*57*). A cholera toxin A1 mutant that lacked lysines and had a blocked N-terminus and therefore could not be polyubiquitinated remained active in vivo. The A1 chain of cholera toxin escapes proteasome-mediated degradation because it contains very few lysine

residues in its primary sequence and rapidly refolds to a stable conformation after entering the cytosol (*57*). When the two lysine residues in RTA were changed to arginines, the stability of RTA was indistinguishable from wild-type RTA, suggesting that its degradation in the cytosol is not ubiquitin mediated. However, when four additional lysines were introduced into RTA, degradation was significantly enhanced, indicating that it is susceptible to proteasome-mediated degradation (*58*). In contrast to RTA, PAP contains 20 lysine residues. Because of the abundance of lysine residues in PAP, it was thought not to undergo retro-translocation into the cytosol (*58*−*59*). We show that the mature form of PAP is extremely stable in the cytosol up to 4 h with no apparent loss. The steady-state analysis indicated that the mature form is stable even up to 24 h (Figure 5). One way PAP may escape degradation is by rapid folding into a stable conformation upon entering the cytosol. Further studies will address the mechanism by which PAP retro-translocates into the cytosol and escapes degradation by the proteasome machinery.

In this study, we show that PAP is localized in the ER in yeast and is retro-translocated from the ER into the cytosol where it depurinates ribosomes and inhibits translation. We present evidence that asparagine 70 in PAP is required for depurination of cytosolic ribosomes. An alteration of this residue prevents ribosome depurination in trans, without altering the ability of the protein to target its own mRNA. The destabilization of mRNA that occurs in yeast expressing N70A takes place in the absence of both cytotoxicity and cell death. These results provide a framework for facilitating rational engineering of other antiviral RIPs with reduced or abolished toxicity. More importantly, we are closer to expressing these less toxic versions of RIPs while still maintaining their therapeutic efficacy.

ACKNOWLEDGMENT

We thank Drs. Aaron Shatkin, Katalin Hudak, and Jon Dinman for critical reading of the manuscript and Drs. Daniel Scott and Randy Schekman for help with microsome isolation, protease protection, and Kar2p antibodies.

REFERENCES

1. Dallal, J. A., and Irvin, J. D. (1978) Enzymatic inactivation of eukaryotic ribosomes by the pokeweed antiviral protein, *FEBS Lett. 89*, 257−259.
2. Endo, Y., and Tsurugi, K. (1987) RNA *N*-glycosidase activity of ricin A-chain. Mechanism of action of the toxic lectin ricin on eukaryotic ribosomes, *J. Biol. Chem. 262*, 8128−8130.
3. Endo, Y., and Tsurugi K. (1988) The RNA *N*-glycosidase activity of ricin A chain. The characteristics of the enzymatic activity of ricin A-chain with ribosome and with rRNA, *J. Biol. Chem. 263*, 8735−8739.
4. Hartley, M. R., Legname, G., Osborn, R., Chen, Z., and Lord, M. J. (1991) Single chain ribosome inactivating proteins from plants depurinate *Escherichia coli* 23S ribosomal RNA, *FEBS Lett. 290*, 65−68.
5. Sandvig, K. (2001) Shiga toxins, *Toxicon 39*, 1629−1635.
6. Hudak, K. A., Wang, P., and Tumer, N. E. (2000) A novel mechanism for inhibition of translation by pokeweed antiviral protein: Depurination of capped RNA template, *RNA 6*, 369−380.
7. Montanaro, L., Sperti, S., Mattioli, A., Testoni, G., and Stirpe, F. (1975) Inhibition by ricin of protein synthesis in vitro. Inhibition of the binding of elongation factor 2 and of adenosine diphosphate-ribosylated elongation factor 2 to ribosomes, *Biochem. J. 146*, 127−131.
8. Taylor, S., Massiah, A., Lomonossoff, G., Roberts, L. M., Lord, J. M., and Hartley, M. (1994) Correlation between the activities of five ribosome-inactivating proteins in depurination of tobacco ribosomes and inhibition of tobacco mosaic virus infection, *Plant J. 5*, 827−835.
9. Wang, P., and Tumer, N. E. (2000) Virus resistance mediated by ribosome inactivating proteins, *Adv. Virus Res. 55*, 325−356.
10. Nielsen, K., and Boston, R. S. (2001) Ribosome inactivating proteins: A Plant Perspective, *Annu. Rev. Plant Physiol. Plant Mol. Biol. 52*, 785−816.
11. Parikh, B. A., and Tumer, N. E. (2004) Antiviral activity of ribosome inactivating proteins in medicine, *Mini-Rev. Med. Chem. 4*, 529−549.
12. Tumer, N. E., Hwang, D. J., and Bonness, M. (1997) C-terminal deletion mutant of pokeweed antiviral protein inhibits viral infection but does not depurinate host ribosomes, *Proc. Natl. Acad. Sci. U.S.A. 94*, 3866−3871.
13. Zoubenko, O., Hudak, K. A., and Tumer, N. E. (2000) A nontoxic pokeweed antiviral protein mutant inhibits pathogen infection via a novel salicylic acid-independent pathway, *Plant Mol. Biol. 44*, 219−229.
14. Uckun, F. M. (1993) Immunotoxins for the treatment of leukemia, *Brit. J. Haematol. 85*, 435−438.
15. Szatrowski, T. P., Dodge, R. K., Reynolds, C., Westbrook, C. A., Frankel, S. R., Sklar, J., Stewart, C. C., Hurd, D. D., Kolitz, J. E., Velez-Garcia, E., Stone, R. M., Bloomfield, C. D., Schiffer, C. A., and Larson, R. A. (2003) Lineage specific treatment of adult patients with acute lymphoblastic leukemia in first remission with anti-B4-blocked ricin or high-dose cytarabine; Cancer and Leukemia Group B Study 9311, *Cancer 97*, 1471−1480.
16. Herrera, L., Yarbrough, S., Ghetie, V., Aquino, D. B., and Vitetta, E. S. (2003) Treatment of SCID/human B cell precursor ALL with anti-CD19 and anti-CD22 immunotoxins, *Leukemia 17*, 334−338.
17. Zapor, M., and Fishbain, J. T. (2004) Aerosolized biologic toxins as agents of warfare and terrorism, *Respir. Care Clin. N. Am. 10*, 111−122.
18. Christopher, G. W., Cieslak, T. J., Pavlin, J. A., and Eitzen, E. M., Jr. (1997) Biological warfare. A historical perspective, *JAMA 278*, 412−417.
19. Monzingo, A. F., Collins, E. J., Ernst, S. R., Irvin, J. D., and Robertus, J. D. (1993) The 2.5 Å structure of pokeweed antiviral protein, *J. Mol. Biol. 233*, 705−715.
20. Ago, H., Kataoka, J., Tsuge, H., Habuka, N., Inagaki, E., Noma, M., and Miyano, M. (1994) X-ray structure of a pokeweed antiviral protein, coded by a new genomic clone, at 0.23 nm resolution. A model structure provides a suitable electrostatic field for substrate binding, *Eur. J. Biochem. 225*, 369−374.
21. Kurinov, I. V., Myers, D. E., Irvin, J. D., and Uckun, F. M. (1999) X-ray crystallographic analysis of the structural basis for the interactions of pokeweed antiviral protein with its active site inhibitor and ribosomal RNA substrate analogs, *Protein Sci. 8*, 1765−1772.
22. Schlossman, D., Withers, D., Welsh, P., Alexander, A., Robertus, J., and Frankel, A. (1989) Role of glutamic acid 177 of the ricin toxin A chain in enzymatic inactivation of ribosomes, *Mol. Cell. Biol. 9*, 5012−5021.
23. Frankel, A., Welsh, P., Richardson, J., and Robertus, J. D. (1990) Role of arginine 180 and glutamic acid 177 of ricin toxin a chain in enzymatic inactivation of ribosomes, *Mol. Cell. Biol. 10*, 6257−6263.
24. Ready, M. P., Kim, Y., and Robertus, J. D. (1991) Site-directed mutagenesis of ricin A chain and implications for the mechanism of action, *Proteins 10*, 270−278.
25. Montfort, W., Villafranca, J., Monzingo, A., Ernst, S., Katzin, B., Rutenber, E., Xuong, N., Hamlin, R., and Robertus, J. (1987) The 3-D structure of ricin at 2.8 Å, *J. Biol. Chem. 262*, 5398−5403.
26. Hudak, K. A., Bauman, J. D., and Tumer, N. E. (2002) Pokeweed antiviral protein binds to the cap structure of eukaryotic mRNA and depurinates the mRNA downstream of the cap, *RNA 8*, 1148−1159.
27. Parikh, B. A., Coetzer, C., and Tumer, N. E. (2002) Pokeweed antiviral protein regulates the stability of its own mRNA by a mechanism that requires depurination but can be separated from depurination of the α-sarcin/ricin loop of rRNA, *J. Biol. Chem. 277*, 41428−41437.
28. Hudak, K. A., Parikh, B. A., Di, R., Baricevic, M., Santana, M., Seskar, M., and Tumer, N. E. (2004) Generation of pokeweed antiviral protein mutations in *Saccharomyces cerevisiae*: Evidence

that ribosome depurination is not sufficient for cytotoxicity, *Nucleic Acids Res. 32*, 4244−4256.
29. Sandvig, K., Garred, O., Prydz, K., Kozlov, J., Hansen, S. H., and van Deurs, B. (1992) Retrograde transport of endocytosed Shiga toxin to the endoplasmic reticulum, *Nature 358*, 510−512.
30. Simpson, J. C., Roberts, L. M., Romisch, K., Davey, J., Wolf, D. H., and Lord, J. M. (1999) Ricin A chain utilizes the endoplasmic reticulum associated protein degradation pathway to enter the cytosol of yeast, *FEBS Lett. 459*, 80−84.
31. Rapak, A., Falsnes, P., and Olsnes, S. (1997) Retrograde transport of mutant ricin to the endoplasmic reticulum with subsequent translocation to cytosol, *Proc. Natl. Acad. Sci. U.S.A. 94*, 3783−3788.
32. Di Cola, A., Frigero, L., Lord, J. M., Ceriotti, A., and Roberts, L. M. (2001) Ricin A chain without its partner B chain is degraded after retrotranslocation from the endoplasmic reticulum to the cytosol in plant cells, *Proc. Natl. Acad. Sci. U.S.A. 98*, 14726−14731.
33. Tsai, B., Ye, Y., and Rapoport, T. A. (2002) Retro-translocation of proteins from the endoplasmic reticulum into the cytosol, *Nature Rev. Mol. Cell. Biol. 3*, 246−255.
34. Wiertz, E. J., Tortorella, D., Bogyo, M., Yu, J., Mothes, W., Jones, T. R., Rapoport, T. A., and Ploegh, H. L. (1996) Sec61-mediated transfer of a membrane protein from the endoplasmic reticulum to the proteasome for destruction, *Nature 384*, 432−438.
35. Lord, J. M., and Roberts, L. M. (1998) Toxin entry: retrograde transport through the secretory pathway, *J. Cell. Biol. 140*, 733−736.
36. Sandvig, K., and van Deurs, B. (2002) Transport of protein toxins into cells: pathways used by ricin, cholera toxin, and Shiga toxin, *FEBS Lett. 529*, 49−53.
37. Hur, Y., Hwang, D. J., Zoubenko, O., Coetzer, C., Uckun, F. M., and Tumer, N. E. (1995) Isolation and characterization of pokeweed antiviral protein mutations in *Saccharomyces cerevisiae*: identification of residues important for toxicity, *Proc. Natl. Acad. Sci. U.S.A. 92*, 8448−8452.
38. Tumer, N. E., Parikh, B. A., Li, P., and Dinman, J. D. (1998) The pokeweed antiviral protein specifically inhibits Ty*1*-directed +1 ribosome frameshifting and retrotransposition in *Saccharomyces cerevisiae*, *J. Virol. 72*, 1036−1042.
39. Glaser, F., Pupko, T., Paz, I., Bell, R. E., Bechor-Shental, D., Martz, E., and Ben-Tal, N. (2003) ConSurf: identification of functional regions in proteins by surface-mapping phylogenetic information, *Bioinformatics 19*, 163−164.
40. Monzingo, A. F., and Robertus, J. D. (1992) X-ray analysis of substrate analogues in the ricin A-chain active site, *J. Mol. Biol. 227*, 1136−1145.
41. Ma, Q. J., Li, J. H., Li, H. G., Wu, S., and Dong, Y. C. (2003) Crystal structure of β-luffin, a ribosome-inactivating protein at 2.0 Å resolution, *Acta Crystallogr., Sect. D. 59*, 1366−1370.
42. Savino, C., Federici, L., Ippoliti, R., Lendaro, E., and Tsernoglou, D. (2000) The crystal structure of saporin SO6 from *Saponaria officinalis* and its interaction with the ribosome, *FEBS Lett. 470*, 239−243.
43. Huang, Q., Liu, S., Tang, Y., Jin, S., and Wang, Y. (1995) Studies on crystal structures, active-center geometry, and depurinating mechanism of two ribosome-inactivating proteins, *Biochem. J. 309*, 285−298.
44. Hudak, K. A., Dinman, J. D., and Tumer, N. E. (1999) Pokeweed antiviral protein accesses ribosomes by binding to L3, *J. Biol. Chem. 274*, 3859−3864.
45. Frey, S., Pool, M., and Seedorf, M. (2001) Scp160p, an RNA-binding, polysome-associated protein, localized to the endoplasmic reticulum of *Saccharomyces cerevisiae* in a microtubule-dependent manner, *J. Biol. Chem. 276*, 15905−15912.
46. Kornitzer, D. (2002) Monitoring protein degradation, *Methods Enzymol. 351*, 639−647.
47. Iizuka, N., and Sarnow, P. (1997) Translation-competent extracts from *Saccharomyces cerevisiae*: effects of L-A RNA 5′ cap and 3′ poly (A) tail on translational efficiency of mRNAs, *Methods 11*, 353−360.
48. Hu, G., Gershon, P. D., Hodel, A. E., and Quiocho, F. A. (1999) mRNA cap recognition: dominant role of enhanced stacking interactions between methylated bases and protein aromatic side chains, *Proc. Natl. Acad. Sci. U.S.A. 96*, 7149−7154.
49. Hudak, K. A., Hammell, A. B., Yasenchak, J., Tumer, N. E., and Dinman, J. D. (2001) A C-terminal deletion mutant of pokeweed antiviral protein inhibits programmed +1 ribosomal frameshifting and Ty*1* retrotransposition without depurinating the sarcin/ricin loop of rRNA, *Virology 279*, 292−301.
50. Rajamohan, F., Pugmire, M. J., Kurinov, I. V., and Uckun, F. M. (2000) Modeling and alanine scanning mutagenesis studies of recombinant pokeweed antiviral protein, *J. Biol. Chem. 275*, 3382−3390.
51. Rajamohan, F., Mao, C., and Uckun, F. M. (2001) Binding interactions between the active-center cleft of recombinant pokeweed antiviral protein and the α-sarcin/ricin stem loop of ribosomal RNA, *J. Biol. Chem. 276*, 24075−24081.
52. Rajamohan, F., Ozer, Z., Mao, C., and Uckun, F. M. (2001) Active center cleft residues of pokeweed antiviral protein mediate its high affinity binding to the ribosomal protein L3, *Biochemistry 40*, 9104−9114.
53. Hiller, M. M., Finger, A., Schweiger, M., and Wolf, D. (1996) ER degradation of a misfolded luminal protein by the cytosolic ubiquitin-proteasome pathway, *Science 273*, 1725−1728.
54. Werner, E. D., Brodsky, J. L., and McCracken, A. A. (1996) Proteasome dependent, endoplasmic reticulum associated protein degradation: an unconventional route to familiar fate, *Proc. Natl. Acad. Sci. U.S.A. 93*, 13792−13801.
55. Hazes, B., and Read, R. J. (1997) Accumulating evidence suggests that several AB toxins subvert the endoplasmic reticulum associated protein degradation pathway to enter target cells, *Biochemistry 36*, 11051−11054.
56. Ng, D. T. W., Brown, J. D., and Walter, P. (1996) Signal sequences specify the targeting route to the endoplasmic reticulum membrane, *J. Cell Biol. 134*, 269−278.
57. Rodighiero, C., Tsai, B., Rapaport, T. A., and Lencer, W. I. (2002) Role of ubiquitination in retro-translocation of cholera toxin and escape of cytosolic degradation, *EMBO Rep. 3*, 1222−1227.
58. Deeks, E. D., Cook, J. P., Day, P. J., Smith, D. C., Roberts, L. M., and Lord, J. M. (2002). The low lysine content of ricin A chain reduces the risk of proteolytic degradation after translocation from the endoplasmic reticulum to the cytosol, *Biochemistry 41*, 3405−3413.
59. Lord, J. M., Deeks, E., Marsden, C. J., Moore, K., Pateman, C., Smith, D. C., Spooner, P., Watson, P., and Roberts, L. M. (2003) Retrograde transport of toxins across the endoplasmic reticulum membrane, *Biochem. Soc. Trans. 31*, 1260−1262.

BI048188C